Fluctuation-dissipation relation and stationary distribution of an exactly solvable many-particle model for active biomatter far from equilibrium

Roland R. Netz
Fachbereich Physik, Freie Universität Berlin, 14195 Berlin, Germany

An exactly solvable, Hamiltonian-based model of many massive particles that are coupled by harmonic potentials and driven by stochastic non-equilibrium forces is introduced. The stationary distribution and the fluctuation-dissipation relation are derived in closed form for the general non-equilibrium case. Deviations from equilibrium are on one hand characterized by the difference of the obtained stationary distribution from the Boltzmann distribution; this is possible because the model derives from a particle Hamiltonian. On the other hand, the difference between the obtained non-equilibrium fluctuation-dissipation relation and the standard equilibrium fluctuation-dissipation theorem allows us to quantify non-equilibrium in an alternative fashion. Both indicators of non-equilibrium behavior, i.e., deviations from the Boltzmann distribution and deviations from the equilibrium fluctuation-dissipation theorem, can be expressed in terms of a single non-equilibrium parameter α that involves the ratio of friction coefficients and random force strengths. The concept of a non-equilibrium effective temperature, which can be defined by the relation between fluctuations and the dissipation, is by comparison with the exactly derived stationary distribution shown not to hold, even if the effective temperature is made frequency dependent. The analysis is not confined to close-to-equilibrium situations but rather is exact and thus holds for arbitrarily large deviations from equilibrium. Also, the suggested harmonic model can be obtained from non-linear mechanical network systems by an expansion in terms of suitably chosen deviatory coordinates; the obtained results should thus be quite general. This is demonstrated by comparison of the derived non-equilibrium fluctuation dissipation relation with experimental data on actin networks that are driven out of equilibrium by energy-consuming protein motors. The comparison is excellent and allows us to extract the non-equilibrium parameter α from experimental spectral response and fluctuation data. © *2018 Author(s). All article content, except where otherwise noted, is licensed under a Creative Commons Attribution (CC BY) license (http://creativecommons.org/licenses/by/4.0/).* https://doi.org/10.1063/1.5020654

INTRODUCTION

Systems that are maintained far from equilibrium are interesting for two reasons: First, nature is not in equilibrium, but rather energy is constantly injected and removed through a cascade of interwoven dissipation levels from astrophysical and geophysical down to biological and microbiological length and time scales. Equilibrium theories, that are commonly used to describe natural processes, thus typically employ idealizations and simplifications. Second, most theoretical models and principles exclusively apply to equilibrium systems, while methods for the description of non-equilibrium situations are less developed, so the study of non-equilibrium phenomena most likely will produce new basic concepts and fundamental insights.[1–4]

There are two distinct ways of characterizing a non-equilibrium system: On the one hand, systems far from equilibrium deviate from the Boltzmann distribution, the founding principle of statistical mechanics. Even phase transitions have been observed as a function of the rate at which energy is injected into a system. Examples include phase separation of particles driven by external[5–10] or internal forces[11–18] and the collective response of pedestrians to spatial

confinement.[19] Experimentally, symmetry-breaking transitions in suspensions of swimming bacteria and filament systems driven by motor proteins have indeed been demonstrated.[20,21] Non-equilibrium shape transformations have been described for polymers driven by externally applied torques.[22,23] For some systems, such effects can be derived by a solution of the governing dynamic equations or by the system's tendency to maximize its dissipation, i.e., its entropy production,[24] but a general understanding of non-equilibrium systems based on distribution function theory is missing.

A fundamentally different indicator of non-equilibrium is a violation of the fluctuation-dissipation theorem (FDT), the key theoretical concept to describe the dynamical response of a system close to equilibrium.[2] According to the FDT, the time derivative of the autocorrelation function of an observable that is coupled to an externally applied time-dependent force is proportional to the linear response function. Modified versions of the FDT that account for non-equilibrium effects have been discussed in the context of laser,[25] chaotic,[26] glassy,[27] colloidal,[28] sheared,[29–31] and active systems.[32–34] Generalized non-equilibrium fluctuation-dissipation relations were derived[25,35–40] and compared with experimental data for glasses,[41] colloids,[42,43] and bundles of biological

filaments.[44,45] These two distinct ways of characterizing non-equilibrium systems, i.e., deviations from the Boltzmann distribution and the breakdown of the FDT, were not linked to each other in the past, simply because of the lack of a suitable model system. The main insight of this paper is derived from an in-depth comparison of these complementary definitions of non-equilibrium for an explicitly solvable particle-based model.

In fact, driven non-equilibrium systems pose a whole number of fundamental questions: What is the relation between FDT violation and deviations from the Boltzmann distribution, are these two indicators of non-equilibrium behavior necessarily coupled, or could—alternatively—only one of them be observed? Why is FDT violation in an experimental system, such as biopolymer networks that are driven by protein motors,[46] typically seen at low frequencies, and is this a property of the active noise spectrum, or rather of the biopolymeric network? Can a non-equilibrium system be described by an effective non-equilibrium temperature and which would preserve the symmetry of the Boltzmann distribution and the structure of the FDT (possibly by introducing a frequency-dependent temperature[4,26,27,32])?

What is needed in order to address these questions is a Hamiltonian-based model that is simple enough to allow for the in-depth analysis of the distribution functions, yet complex enough to yield non-trivial response functions, and that can be continuously moved away from equilibrium by a suitable control parameter. We here introduce such a model, which consists of n massive active particles that are elastically coupled to a central particle, as schematically depicted in Fig. 1. Each particle is coupled to a heat sink via friction and subject to a stochastic force that drives the system away from equilibrium.

Our theoretical model is motivated by the experimental system of an actin network in the presence of myosin motor proteins, for which a stark FDT violation has been demonstrated at increased adenosine triphosphate (ATP, the molecular energy unit in biology) concentration.[46] In these experiments, the FDT has been explicitly checked by simultaneously measuring the spatial autocorrelation of a colloidal bead and the response of the bead to an externally applied force.[47,48]
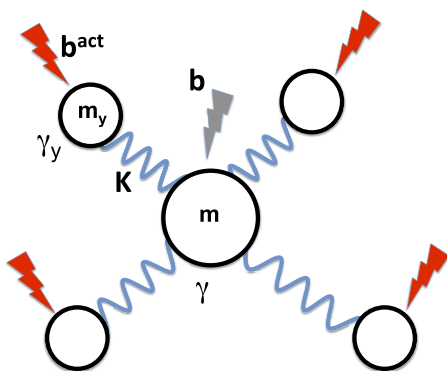

FIG. 1. In the model based on the Hamiltonian Eq. (1), n particles of mass m_y and with friction coefficient γ_y are elastically coupled to a central particle that has mass m and friction coefficient γ. The harmonic springs have a strength of K. The n peripheral particles are subject to random forces of strength b^{act} which are tuned to induce non-equilibrium behavior; the central particle is subject to a random force of strength b.

In the absence of motor activity, the FDT was demonstrated to be perfectly obeyed; for ATP-induced motor activity, the FDT was significantly violated at low frequencies where the bead fluctuations were seen to be much larger than the bead response.[46] In our comparison with the experimental data, the central particle represents the colloidal probe, while the active particles are the protein motors that are mechanically coupled to the central particle by actin filaments.

Similar models have been studied before in the classical[27,37,49] and quantum[50] equilibrium cases in order to understand how friction and memory effects arise from coupled many-particle systems. Such many-particle models have also been studied in the non-equilibrium situation where different particles are coupled to thermal baths with different temperatures, and effective temperatures were derived from the calculated fluctuation-dissipation relations and compared to stationary distributions.[51,52] The main advantage of our model is that on the one hand the stationary distribution can be calculated explicitly by mapping on the Fokker-Planck equation, and on the other hand, the response and autocorrelation functions can be obtained from the conjugated generalized Langevin equation. We show that a non-Boltzmann stationary distribution and FDT violation occur hand in hand and are described by a single parameter which quantifies departure from equilibrium, denoted as α. We derive the non-equilibrium FDT which allows the quantitative description of the experimental frequency-dependent motion of a tracer bead in an ATP driven actin network.[46] By the mapping of our model on the experimental spectral data,[46] we extract for the non-equilibrium parameter the value $\alpha = 20$, which we interpret in terms of physical parameters such as friction coefficients, particle masses, and the input power of motor units. The high value of α indicates that the experimental system is far from equilibrium. The main strength of our harmonic model is that, due to its simple nature, it allows us to derive the stationary distribution and the fluctuation-dissipation relation in an exact manner, i.e., arbitrarily far away from equilibrium. As a main insight, our results demonstrate that the concept of a non-equilibrium effective temperature has only a rather limited validity since the effective temperature that is extracted from the generalized non-equilibrium fluctuation-dissipation relation is different from the effective temperature one would derive from the non-equilibrium stationary distribution, regardless of how far from equilibrium the system is moved. In fact, even an arbitrarily small non-equilibrium forcing breaks the symmetry of the stationary distribution, vividly demonstrated by couplings between particle velocities and positions, which in equilibrium are absent.

Clearly, a harmonic model can always be obtained from a more complex, non-linear mechanical network by a Gaussian expansion in terms of suitably defined deviatory coordinates. Our model should thus quite generally describe mechanical systems far from equilibrium, as long as the mechanical response is close to linear, even when the system is far from equilibrium as described by our non-equilibrium parameter α. This expectation is confirmed by the good comparison of our model with experimental spectral data for driven actin biopolymeric networks.

STATIONARY DISTRIBUTION OF MANY-PARTICLE MODEL

To proceed, we consider a tracer particle of mass m that is via harmonic bonds of strength K coupled to n active particles of mass m_y. The Hamiltonian is given by

$$H = \frac{K_x}{2}x^2 + \frac{m}{2}v^2 + \sum_{i=1}^{n}\frac{K}{2}(x - y_i)^2 + \sum_{i=1}^{n}\frac{m_y}{2}w_i^2, \quad (1)$$

where x and v are the position and the velocity of the tracer bead while y_i and w_i are the positions and velocities of the active particles, respectively. The central particle is in addition confined by a harmonic potential of strength K_x. Our one-dimensional model can be trivially generalized to three dimensions. By adding friction terms and random forces to the Hamilton equations, which mimics the presence of a heat bath, we obtain the coupled set of linear Langevin equations

$$\dot{x}(t) = v(t),$$
$$m\,\dot{v}(t) = -\gamma v(t) - (nK + K_x)x(t) + K\sum_i y_i(t) + bF_v(t),$$
$$\dot{y}_i(t) = w_i(t),$$
$$m_y\,\dot{w}_i(t) = -\gamma_y w_i(t) - K(y_i(t) - x(t)) + b_i^{act}F_i^{act}(t),$$
(2)

where γ is the friction coefficient of the tracer bead and γ_y is the friction coefficient of the active particles. For simplicity, we assume Gaussian random forces with zero mean and variances $\langle F_v(t)F_v(t')\rangle = 2\delta(t - t')$ and $\langle F_i^{act}(t)F_j^{act}(t')\rangle = 2\delta_{ij}\delta(t - t')$; the random force strengths are b for the tracer bead and b_i^{act} for the active particles. Note that for an equilibrium system one would now fix the noise strengths at values $b^2 = k_BT\gamma$ for the tracer bead and $(b_i^{act})^2 = k_BT\gamma_y$ for the active particles in order to recover Maxwell-Boltzmann distributions for the velocities.[53] We do not do this, but rather analyze the model for arbitrary random force strengths. Summing over the equations for the active particles, we arrive at the reduced Langevin equations

$$\dot{x}(t) = v(t),$$
$$m\,\dot{v}(t) = -\gamma v(t) - K_x x(t) + nK(y(t) - x(t)) + bF_v(t),$$
$$\dot{y}(t) = w(t),$$
$$m_y\,\dot{w}(t) = -\gamma_y w(t) - K(y(t) - x(t)) + b_y F_w(t),$$
(3)

where we defined the mean position and velocity of the active particles as $y(t) = \sum_i y_i(t)/n$ and $w(t) = \sum_i w_i(t)/n$, respectively. The random force acting on the mean position of the active particles is given by

$$F_w(t) = \sum_{i=1}^{n}\frac{b_i^{act}F_i^{act}(t)}{nb_y}, \quad (4)$$

with $b_y^2 = \sum_i(b_i^{act})^2/n^2$ and satisfies $\langle F_w(t)F_w(t')\rangle = 2\delta(t - t')$. The set of linear stochastic differential equations defined by Eq. (3) can be written as a matrix equation

$$\dot{z}_k(t) = -A_{km}z_m(t) + \Phi_{km}F_m(t), \quad (5)$$

where we defined the four-dimensional state vector $\vec{z}(t) = (x(t), v(t), y(t), w(t))$ and the random force vector $\vec{F}(t) = (F_x(t), F_v(t), F_y(t), F_w(t))$. Note that doubly appearing indices are summed over. The matrices appearing in Eq. (5) are given explicitly by

$$A = \begin{pmatrix} 0 & -1 & 0 & 0 \\ nK/m + K_x/m & \gamma/m & -nK/m & 0 \\ 0 & 0 & 0 & -1 \\ -K/m_y & 0 & K/m_y & \gamma_y/m_y \end{pmatrix} \quad (6)$$

and

$$\Phi = \begin{pmatrix} 0 & 0 & 0 & 0 \\ 0 & b/m & 0 & 0 \\ 0 & 0 & 0 & 0 \\ 0 & 0 & 0 & b_y/m_y \end{pmatrix}. \quad (7)$$

The associated Fokker-Planck equation for the time-dependent density distribution $P(\vec{z}, t) = P(x, v, y, w, t)$ follows via the Kramers-Moyal expansion of Eq. (5) as[53]

$$\dot{P}(\vec{z}, t) = [\nabla_k A_{km}z_m + \nabla_k\nabla_m C_{km}]P(\vec{z}, t), \quad (8)$$

where $C_{ij} = \Phi_{ik}\Phi_{jk}$. With the Gaussian ansatz for the stationary distribution

$$P_0(\vec{z}) = \mathcal{N}^{-1}\exp(-z_i E_{ij}^{-1}z_j/2), \quad (9)$$

where $\mathcal{N}$ is an unimportant normalization constant, we obtain from Eq. (8) and the stationarity condition $\dot{P}(\vec{z}, t) = 0$ the following equation:

$$A_{ii} - A_{ij}z_j E_{ik}^{-1}z_k + C_{ij}(E_{ik}^{-1}z_k E_{jl}^{-1}z_l - E_{ij}^{-1}) = 0. \quad (10)$$

This is equivalent to the Lyapunov equation

$$A_{ik}E_{kj} + A_{jk}E_{ki} = 2C_{ij}, \quad (11)$$

as shown in the supplementary material, where we also present the explicit solution for all entries of the covariance matrix E_{ij}, which is easily found by solving the set of linear equations defined by Eq. (11). We note that $E_{xv} = \langle xv\rangle = 0$ and $E_{yw} = \langle yw\rangle = 0$ and that $\langle xw\rangle = -\langle yv\rangle$, irrespective of the parameters, which reduces the number of independent covariances from ten (for a symmetric four-by-four matrix) down to seven. For the remaining seven covariances, a fundamental symmetry transpires: if the noise strengths acting on the active and tracer particles, b_y and b, respectively, obey the relation

$$b_y^2 = b^2\gamma_y/(n\gamma), \quad (12)$$

we obtain as stationary solution the simple result

$$P_0 \simeq \exp(-\gamma H/b^2), \quad (13)$$

where H is the Hamiltonian defined in Eq. (1). Thus, ordinary Boltzmann statistics is recovered if the noise strength acting on the tracer particle is chosen as $b^2 = \gamma k_BT$, in which case one obtains $P_0 \simeq \exp(-H/k_BT)$. If Eq. (12) holds, we explicitly find $\langle v^2\rangle = k_BT/m$, $\langle w^2\rangle = k_BT/(nm_y)$, $\langle x^2\rangle = k_BT/K_x$, $\langle y^2\rangle = k_BT(1/K_x + 1/(nK))$, $\langle(x - y)^2\rangle = k_BT/(nK)$, and $\langle xw\rangle = \langle yv\rangle = \langle vw\rangle = 0$ (as shown in the supplementary material). This is precisely what one would derive from standard

equilibrium statistical mechanics. To quantify the departure from equilibrium, we define the non-equilibrium parameter α as

$$b_y^2 = (1 + \alpha)b^2\gamma_y/(n\gamma). \tag{14}$$

For $\alpha = 0$, we recover Eq. (12) and thus the equilibrium stationary distribution. For $\alpha \neq 0$, we obtain a non-equilibrium stationary distribution that is characterized by non-vanishing couplings between velocities and positions that are linearly proportional to α, $\langle xw \rangle = -\langle yv \rangle \propto \alpha$ as well as $\langle vw \rangle \propto \alpha$, and positional covariances that deviate from the equilibrium solution. The complete and exact stationary non-equilibrium solution is shown in the supplementary material; due to the length of the resulting expressions, we exemplarily show here only positional variances in the vanishing mass (i.e., overdamped) limit $m = m_y = 0$,

$$\langle x^2 \rangle = \frac{k_B T}{K_x}\left(1 + \frac{\alpha n\gamma_y}{n\gamma_y + \gamma + \gamma_y K_x/K}\right), \tag{15}$$

$$\langle (x - y)^2 \rangle = \frac{k_B T}{nK}\left(1 + \alpha\frac{K\gamma + K_x\gamma_y}{K\gamma + K_x\gamma_y + nK\gamma_y}\right). \tag{16}$$

The following properties are noteworthy:

(i) For $\alpha = 0$, the second term in the parentheses vanishes and thus the equilibrium result for the mean-square displacement of a particle in a harmonic potential of strength K_x or nK, the first term, is recovered.

(ii) For active particles into which the random forces inject more energy than in equilibrium, i.e., for $\alpha > 0$, the tracer particle is less confined and the variance $\langle x^2 \rangle$ in Eq. (15) goes up; this effect is linear in α. Likewise, the variance $\langle (x - y)^2 \rangle$ in Eq. (16) increases linearly with α.

(iii) Although it is vital to consider the complete Fokker-Planck equation with finite particle masses since this allows us to observe the symmetry breaking of the stationary distribution for $\alpha \neq 0$ in terms of velocity-position correlations very clearly, non-equilibrium effects survive in the overdamped, mass-less limit.

(iv) In the absence of elastic coupling between tracer and active particles, i.e., for $K = 0$, the non-equilibrium effect on $\langle x^2 \rangle$ in Eq. (15) (not surprisingly) vanishes.

(v) The limit of vanishing friction is somewhat subtle, and the behavior depends on how this limit is approached; for example, if $\gamma \to 0$ and $\gamma_y \to 0$ at a constant ratio γ/γ_y, the non-equilibrium effect on the variances does not vanish.

(vi) Finally, for vanishing confinement potential of the tracer particle, i.e., for $K_x = 0$, the variance $\langle x^2 \rangle$ in Eq. (15) is infinity regardless of the value of α; we thus see that active particles cannot confine a particle, that in equilibrium is unconfined (which is a consequence of spatial homogeneity). Likewise, the variance $\langle (x - y)^2 \rangle$ in Eq. (16) is for $K = 0$ infinity regardless of the value of α.

We conclude this section by saying that non-equilibrium in our model is quantified by a single parameter α, defined in Eq. (14), which depends on the ratio of friction coefficients and noise strengths acting on the particles. For $\alpha \neq 0$, a symmetry-breaking transition of the stationary solution and a departure from the equilibrium Boltzmann distribution are obtained. We can straightforwardly recognize the non-equilibrium nature of the distribution for $\alpha \neq 0$ because our model is based on a Hamiltonian, and thus the equilibrium distribution is directly given by the Boltzmann weight Eq. (13). This is a significant advantage of our approach that is Hamiltonian based, compared to alternative approaches that start from a dynamic evolution equation.

NON-EQUILIBRIUM FLUCTUATION-DISSIPATION RELATION

We now connect to the experimentally observed FDT violation. For this, we need to calculate autocorrelation functions and response functions; this is most conveniently done using the Langevin equation derived earlier. For simplicity and in order to cast our results for the tracer-bead motion in the form of a generalized Langevin equation, we set the active particle mass to zero, $m_y = 0$. We have seen that this does not eliminate non-equilibrium effects, as the particle positions deviate from the Boltzmann distribution also in the overdamped case, as demonstrated in Eq. (15).

The explicit solution of the Langevin equation (3) for the active particle motion, described by the variable $y(t)$, for $m_y = 0$ reads as

$$y(t) = \int_{-\infty}^{t} dt' e^{-(t-t')K/\gamma_y}\left[\frac{K}{\gamma_y}x(t') + \frac{b_y}{\gamma_y}F_w(t')\right]. \tag{17}$$

Inserting this solution into the Langevin equation (3) for the tracer particle, described by the variables $x(t)$ and $v(t)$, we obtain the generalized Langevin equation

$$m\dot{v}(t) = -K_x x(t) - \int_{-\infty}^{\infty} dt' \Gamma(t - t')v(t') + F(t) + F_{ext}(t), \tag{18}$$

where $F_{ext}(t)$ is an external force which we added for later derivation of the response function. The memory function that appears in Eq. (18) is given by

$$\Gamma(t) = \theta(t)\left[2\gamma\delta(t) + nKe^{-tK/\gamma_y}\right], \tag{19}$$

where $\theta(t)$ denotes the theta function with the properties $\theta(t) = 1$ for $t > 0$ and $\theta(t) = 0$ for $t < 0$, which makes the memory function single sided. The noise $F(t)$ in Eq. (18) is given by

$$F(t) = bF_v(t) + \frac{nKb_y}{\gamma_y}\int_{-\infty}^{t} dt' e^{-(t-t')K/\gamma_y}F_w(t') \tag{20}$$

and consists of the noise acting directly on the tracer particles (proportional to b) and a term due to the noise acting on the active particles (proportional to b_y). The latter term consists of a convolution integral because this noise is transmitted via the elastic linkers of strength K. Defining the auto-correlation function of the random noise as $C_{FF}(t) = \langle F(0)F(t) \rangle$, we obtain

$$C_{FF}(t) = k_B T\left[2\gamma\delta(t) + n(1 + \alpha)Ke^{-|t|K/\gamma_y}\right]. \tag{21}$$

Comparing Eqs. (19) and (21), we see that $C_{FF}(t) = k_B T\Gamma(|t|)$, a consequence of the standard fluctuation-dissipation theorem,[53] only holds for $\alpha = 0$, and for $\alpha \neq 0$ the two functions differ, which points to FDT violation. The memory

function $\Gamma(t)$ and the random-force autocorrelation function $C_{\mathrm{FF}}(t)$ are not directly measurable, and in order to connect to experiments, we need to calculate response functions and particle positional autocorrelation functions. The response function $\chi(t)$ is defined via the particle positional response to an externally applied force

$$x(t) = \int_{-\infty}^{\infty} dt' \chi(t - t') F_{\mathrm{ext}}(t'), \qquad (22)$$

where causality demands $\chi(t) = 0$ for $t < 0$. From the Fourier-transformed generalized Langevin equation (18)

$$\tilde{x}(\omega) = \int dt e^{-i\omega t} x(t) = \tilde{\chi}(\omega)\left[\tilde{F}(\omega) + \tilde{F}_{\mathrm{ext}}(\omega)\right], \qquad (23)$$

we obtain, by averaging over the noise, $\langle\tilde{x}(\omega)\rangle = \tilde{\chi}(\omega)\tilde{F}_{\mathrm{ext}}(\omega)$ and therefore the response function

$$\tilde{\chi}(\omega) = \frac{\langle\tilde{x}(\omega)\rangle}{\tilde{F}_{\mathrm{ext}}(\omega)} = \left[K_x - \omega^2 m + i\omega\tilde{\Gamma}(\omega)\right]^{-1}. \qquad (24)$$

The Fourier transform of the positional autocorrelation function $C_{\mathrm{xx}}(t) = \langle x(0)x(t)\rangle$ is from Eq. (23) and setting the external force to zero given by

$$\tilde{C}_{\mathrm{xx}}(\omega) = \tilde{C}_{\mathrm{FF}}(\omega)\tilde{\chi}(\omega)\tilde{\chi}(-\omega). \qquad (25)$$

The equilibrium FDT reads in the time domain $\chi(t) = -\theta(t)\dot{C}_{\mathrm{xx}}(t)/(k_{\mathrm{B}}T)$, from which we obtain via Fourier transform the standard result for the imaginary part of the response function[53]

$$\tilde{\chi}^I(\omega) = -\omega\tilde{C}_{\mathrm{xx}}(\omega)/(2k_{\mathrm{B}}T). \qquad (26)$$

From Eq. (24), we see that

$$\tilde{\chi}^I(\omega) = -\omega\tilde{\Gamma}^R(\omega)\tilde{\chi}(\omega)\tilde{\chi}(-\omega). \qquad (27)$$

Combining Eqs. (25) and (27), we obtain that

$$\frac{-\omega\tilde{C}_{\mathrm{xx}}(\omega)/(2k_{\mathrm{B}}T)}{\tilde{\chi}^I(\omega)} = \frac{\tilde{C}_{\mathrm{FF}}(\omega)/(2k_{\mathrm{B}}T)}{\tilde{\Gamma}^R(\omega)} \equiv 1 + \Xi(\omega), \qquad (28)$$

where in the last step, we introduced the spectral function $\Xi(\omega)$ that quantifies deviations from the standard FDT shown in Eq. (26). Equation (28) corresponds to the generalized, exact FDT and is valid arbitrarily far away from equilibrium. The Fourier-transformed real part of the memory kernel and random force autocorrelation function follow from Eqs. (19) and (21) as

$$\tilde{\Gamma}^R(\omega) = \gamma + \frac{n\gamma_y}{1 + \omega^2\gamma_y^2/K^2} \qquad (29)$$

and

$$\tilde{C}_{\mathrm{FF}}(\omega)/(2k_{\mathrm{B}}T) = \gamma + \frac{n(1 + \alpha)\gamma_y}{1 + \omega^2\gamma_y^2/K^2}. \qquad (30)$$

By inserting these expressions into the generalized FDT in Eq. (28), we finally obtain for $\Xi(\omega)$ the explicit result

$$\Xi(\omega) = \frac{\alpha n\gamma_y}{n\gamma_y + \gamma + \gamma\gamma_y^2\omega^2/K^2} \simeq \frac{\alpha}{1 + \tau^2\omega^2}, \qquad (31)$$

where in the last step, we made the approximate assumption that $n\gamma_y > \gamma$, which means that the friction coefficient of the
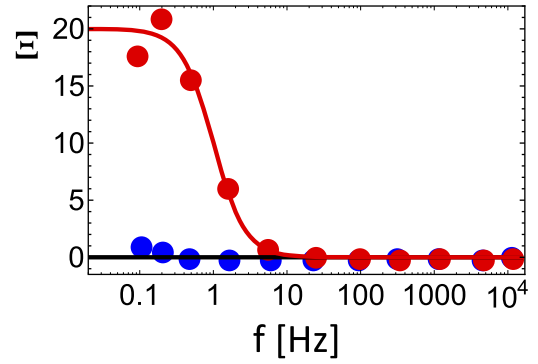

FIG. 2. The spectral function $\Xi(\omega)$ plotted here as a function of frequency $f = \omega/(2\pi)$ characterizes deviations from the equilibrium fluctuation-dissipation theorem and is defined in Eq. (28). Experimental data from motor-protein driven actin networks in the presence of ATP (red circles)[46] are compared with the prediction of Eq. (31) (red line), the extracted non-equilibrium parameter is $\alpha = 20$, and the time scale is $\tau = 1$ s. Blue circles denote experimental results in the absence of myosin motors[46] and agree with the expected equilibrium limit $\Xi(\omega) = 0$ (black horizontal line).

active particles γ_y (which includes half of the physical linker molecules connecting active particles to the tracer bead) times the number of active particles n is larger than the friction coefficient γ of the tracer particle, which is certainly a sensible limit to take. Interestingly, the final result for $\Xi(\omega)$ is not proportional to the number of active particles n; this result can be traced back to our model assumption that the noise acting on different active particles is uncorrelated. The relaxation time defined in Eq. (31) is given by

$$\tau^2 = \frac{\gamma_y\gamma}{nK^2}. \qquad (32)$$

We see that the final expression for the non-equilibrium FDT correction term $\Xi(\omega)$ is of a surprisingly simple Lorentz form and in fact linearly proportional to the non-equilibrium coefficient α. This allows for direct comparison with experiments and, in particular, for extracting α as well as τ from experimental data.

In Fig. 2, we compare $\Xi(\omega)$, defined in Eq. (28) and calculated from experimental data for $\tilde{C}_{\mathrm{xx}}(\omega)$ and $\tilde{\chi}^I(\omega)$ obtained for actin networks with added myosin motors in the presence of ATP (red data points),[46] with the Lorentz scaling form in Eq. (31) (red line). The general agreement between the experimental data and the predicted functional form of $\Xi(\omega)$ is very good; the extracted fitting parameters are $\alpha = 20$ for the non-equilibrium parameter and $\tau = 1$ s for the relaxation time scale. The blue circles represent data that are obtained in the absence of myosin motors and closely agree with the expected result $\Xi(\omega) = 0$ (black horizontal line). The large fit result for α shows that the experimental system is far from equilibrium and thus a non-perturbative treatment of non-equilibrium effects, as accomplished in our calculation, is needed; the value of the relaxation time τ will be interpreted in the section titled Discussion.

DISCUSSION

By the comparison with experimental data in Fig. 2, we see that the derived generalized FDT Eq. (28) works well even

for complex active biological systems. The advantage of our model is that all terms have physical meaning.

To demonstrate this, we first connect the non-equilibrium parameter α to the injected power due to active particles. For this, we consider the Langevin equation for a single active particle in the absence of coupling to the tracer particle (i.e., for $K = 0$), which follows from Eq. (2) as

$$m_y \ddot{y}_i(t) = -\gamma_y \dot{y}_i(t) + b_i^{\text{act}} F_i^{\text{act}}(t). \tag{33}$$

Multiplying by $\dot{y}_i(t)$ and averaging, we obtain

$$\frac{d}{dt} \langle \frac{m_y}{2} \dot{y}_i^2 \rangle = 0 = -\gamma_y \langle \dot{y}_i^2 \rangle + b_i^{\text{act}} \langle \dot{y}_i F_i^{\text{act}} \rangle. \tag{34}$$

The left side is the time derivative of the average kinetic energy of the particle; the right side is the difference of the dissipation rate

$$I = \gamma_y \langle \dot{y}_i^2 \rangle \tag{35}$$

and the injected power

$$P = b_i^{\text{act}} \langle \dot{y}_i F_i^{\text{act}} \rangle. \tag{36}$$

In a stationary state, the injected power is equal to the dissipation rate, and we have $P = I$. We explicitly obtain for the dissipation rate (see the supplementary material)

$$I = \gamma_y \langle \dot{y}_i^2 \rangle = \frac{(1 + \alpha) k_B T \gamma_y}{m_y}, \tag{37}$$

which contains an equilibrium dissipation (independent of α) and a non-equilibrium part proportional to α. We see that both finite mass m_y and finite friction coefficient γ_y are needed in order to make a meaningful comparison of the non-equilibrium parameter α and the dissipation rate I. For the mass of the active particle, we assume $m_y = 4\pi R^3 \rho/3$ with water density $\rho = 10^3$ kg/m³, and for the friction coefficient, we take the Stokes expression $\gamma_y = 6\pi\eta R$ with water viscosity $\eta = 10^{-3}$ Pa s. For the ratio γ_y/m_y, we thus obtain, assuming a typical radius $R = 1$ μm, the value $\gamma_y/m_y = 4 \cdot 10^6$ s⁻¹. We note that the radius R of course includes half of the linker that connects the active particles to the central tracer bead, which explains why we use a rather large value for R in our simple estimate. In terms of the dissipation rate I, our result for γ_y/m_y implies that in order to reach a non-equilibrium parameter of $\alpha = 1$, Eq. (37) predicts that we need to inject a power of $P = I = 8 \cdot 10^6 k_B T$/s; this is quite enormous, considering that typical biological motors consume of the order of 100 ATP/s and that the excess free energy of an ATP molecule is about $30 k_B T$ under physiological conditions.[54] In the experiment shown in Fig. 2, most likely many motors act in parallel on one active unit, which increases the injected power proportionally.

We finally discuss the time scale τ defined in Eq. (32) and that appears in the Lorentz form Eq. (31). Assuming the harmonic coupling potential between active particles and tracer bead to arise from the perpendicular bending of a semi-flexible filament, the harmonic strength is $K \simeq k_B T \ell_P/L^3$,[55] where L denotes the filament length and ℓ_P the persistence length. For the friction coefficient, we again assume $\gamma_y \simeq \gamma \simeq 6\pi\eta R$. Choosing all length scales to be of the order of a micrometer, $\ell_P \simeq L \simeq R \simeq 1$ μm, we obtain from Eq. (32) for the time scale

$\tau \simeq 5/\sqrt{n}$ s. The effective time scale thus depends weakly on n, the number of active units that are coupled to the tracer bead, and should be of the order of a second, in agreement with the fit to the experimental data in Fig. 2. We conclude that the fit parameters extracted in Fig. 2 make sense when interpreted physically. In future experimental studies, it will be interesting to see how α and τ change when experimental parameters such as ATP concentration, motor, and filament density are varied.

CONCLUSION

We have introduced an exactly solvable, Hamiltonian-based many-particle model that accounts for non-equilibrium stochastic driving as well as friction dissipation. On the one hand, by mapping onto a Fokker-Planck equation and solving the stationary distribution in closed form, we characterize the departure from equilibrium by comparison with the Boltzmann distribution. On the other hand, the exact solution of the conjugated Langevin equation allows us to derive a generalized non-equilibrium fluctuation-dissipation relation and thereby to characterize deviations from equilibrium by comparison with the standard equilibrium FDT. Both the stationary distribution and the fluctuation-dissipation relation indicate departures from equilibrium as soon as the non-equilibrium parameter α is non-zero, and thus these two fundamental indicators of non-equilibrium behavior are coupled to each other.

We characterize departures from the equilibrium FDT by the experimentally measurable spectral function $\Xi(\omega)$, defined in Eq. (28), which has Lorentz form in the limit of many active particles, as seen in Eq. (31), in excellent agreement with experimental measurements on active filamentous networks, as shown in Fig. 2. $\Xi(\omega)$ depends on the coupling between active particles and tracer bead as well as on the non-equilibrium driving strength, and it thus offers a spectral fingerprint of non-equilibrium systems. The non-equilibrium fluctuation-dissipation relation Eq. (28) can obviously be interpreted in terms of a frequency-dependent effective temperature, defined by

$$k_B T_{\text{eff}} \equiv k_B T (1 + \Xi(\omega)), \tag{38}$$

by which the standard equilibrium FDT Eq. (26) would be reinstalled by simply using $k_B T_{\text{eff}}$ instead of $k_B T$. However, this fix falls short of describing the non-equilibrium system in its entirety. This is illustrated by the fact that the non-equilibrium stationary distribution does not only differ from the Boltzmann distribution by a factor in the exponential, which would amount to an effective temperature, but rather shows a fundamentally different symmetry: As soon as the non-equilibrium parameter α becomes non-zero, the covariances that couple positions to velocities $\langle xw \rangle = -\langle yv \rangle$ and the velocities of the tracer and active particles $\langle vw \rangle$, which vanish in equilibrium, become non-zero. This cannot be explained by an effective unique temperature, regardless of its definition. Even if we would introduce multiple effective temperatures that are different for each entry in the covariance matrix, the effective temperatures defined by the non-equilibrium

stationary distribution would have to be different from the effective temperatures defined by the generalized fluctuation-dissipation relation, as a comparison of the result for the expectation value for $\langle x^2 \rangle$ in Eq. (15) and the spectral function in Eq. (31) shows. Thus we conclude that the concept of an effective temperature, defined by the non-equilibrium fluctuation-dissipation relation, fails to describe the stationary non-equilibrium distribution and thus has only limited power as a general concept to characterize non-equilibrium systems.

Our model is based on a harmonic Hamiltonian, given in Eq. (1). The generalization to the most general quadratic Hamiltonian with different coupling constants between the active particles and the tracer bead is straightforward but does not change the resulting physics. Non-linear coupling terms are much more difficult to include. We note that our harmonic Hamiltonian can be derived from more general non-linear models by a saddle-point analysis in terms of suitably defined coordinates, so we argue that to leading order in a systematic saddle-point expansion, our model results apply to a wide class of more complicated non-linear models. As a generalization of our model, it would be interesting to include also couplings between particle velocities, which would mimic viscoelastic and hydrodynamic interaction effects.

SUPPLEMENTARY MATERIAL

See supplementary material for details of the derivation and the stationary solution of the Lyapunov equation and the estimate of the injected power.

ACKNOWLEDGMENTS

[1] S. Ramaswamy, Annu. Rev. Condens. Matter Phys. **1**, 323 (2010).
[2] M. Baiesi and C. Maes, New J. Phys. **15**, 013004 (2013).
[3] C. Bechinger, R. Di Leonardo, H. Löwen, C. Reichardt, G. Volpe, and G. Volpe, Rev. Mod. Phys. **88**, 045006 (2016).
[4] A. Puglisi, A. Sarracino, and A. Vulpiani, Phys. Rep. **709**, 1 (2017).
[5] S. Katz, J. L. Lebowitz, and H. Spohn, Phys. Rev. B **28**, 1655 (1983).
[6] J. Krug, Phys. Rev. Lett. **67**, 1882 (1991).
[7] B. Schmittmann and R. K. P. Zia, Phys. Rep. **301**, 45 (1998).
[8] J. Dzubiella, G. P. Hoffmann, and H. Löwen, Phys. Rev. E **65**, 021402 (2002).
[9] R. R. Netz, Europhys. Lett. **63**, 616 (2003).
[10] N. Kumar, H. Soni, S. Ramaswamy, and A. Sood, Nat. Commun. **5**, 4688 (2014).
[11] E. Bertin, M. Droz, and G. Grégoire, Phys. Rev. E **74**, 022101 (2006).
[12] I. Theurkauff, C. Cottin-Bizonne, J. Palacci, C. Ybert, and L. Bocquet, Phys. Rev. Lett. **108**, 268303 (2012).
[13] R. Golestanian, Phys. Rev. Lett. **108**, 038303 (2012).
[14] T. Speck, J. Bialke, A. M. Menzel, and H. Löwen, Phys. Rev. Lett. **112**, 218304 (2014).
[15] F. Ginot, I. Theurkauff, D. Levis, C. Ybert, L. Bocquet, L. Berthier, and C. Cottin-Bizonne, Phys. Rev. X **5**, 011004 (2015).
[16] A. Y. Grosberg and J.-F. Joanny, Phys. Rev. E **92**, 032118 (2015).
[17] S. N. Weber, C. A. Weber, and E. Frey, Phys. Rev. Lett. **116**, 058301 (2016).
[18] H. Tanaka, A. A. Lee, and M. P. Brenner, Phys. Rev. Fluids **2**, 043103 (2017).
[19] D. Helbing, Rev. Mod. Phys. **73**, 1067 (2001).
[20] A. Sokolov, I. S. Aranson, J. O. Kessler, and R. E. Goldstein, Phys. Rev. Lett. **98**, 158102 (2007).
[21] R. Suzuki and A. R. Bausch, Nat. Commun. **8**, 41 (2017).
[22] C. W. Wolgemuth, T. R. Powers, and R. E. Goldstein, Phys. Rev. Lett. **84**, 1623 (2000).
[23] H. Wada and R. R. Netz, Europhys. Lett. **87**, 38001 (2009).
[24] S. R. de Groot and P. Mazur, *Non-Equilibrium Thermodynamics* (North-Holland Publishing Co., Amsterdam, 1962).
[25] G. S. Agarwal, Z. Phys. A: Hadrons Nucl. **252**, 25 (1972).
[26] P. C. Hohenberg and B. I. Shraiman, Phys. D **37**, 109 (1989).
[27] L. F. Cugliandolo, J. Kurchan, and L. Peliti, Phys. Rev. E **55**, 3898 (1997).
[28] T. Speck and U. Seifert, Europhys. Lett. **74**, 391 (2006).
[29] N. Xu and C. S. O'Hern, Phys. Rev. Lett. **94**, 055701 (2005).
[30] D. Levis and L. Berthier, Europhys. Lett. **111**, 60006 (2015).
[31] M. Krüger and M. Fuchs, Phys. Rev. Lett. **102**, 135701 (2009).
[32] D. Loi, S. Mossa, and L. F. Cugliandolo, Phys. Rev. E **77**, 051111 (2008).
[33] A. Suma, G. Gonnella, G. Laghezza, A. Lamura, A. Mossa, and L. F. Cugliandolo, Phys. Rev. E **90**, 052130 (2014).
[34] P. Ilg and J.-L. Barrat, Europhys. Lett. **79**, 26001 (2007).
[35] T. Harada and S. Sasa, Phys. Rev. Lett. **95**, 130602 (2005).
[36] F. Zamponi, F. Bonetto, L. F. Cugliandolo, and J. Kurchan, J. Stat. Mech.: Theory Exp. **2005**, P09013.
[37] J. Prost, J.-F. Joanny, and J. M. R. Parrondo, Phys. Rev. Lett. **103**, 090601 (2009).
[38] M. Baiesi, C. Maes, and B. Wynants, Phys. Rev. Lett. **103**, 010602 (2009).
[39] U. Seifert and T. Speck, Europhys. Lett. **89**, 10007 (2010).
[40] L. Willareth, I. M. Sokolov, Y. Roichman, and B. Lindner, Europhys. Lett. **118**, 20001 (2017).
[41] S. Jabbari-Farouji, D. Mizuno, D. Derks, G. H. Wegdam, F. C. MacKintosh, C. F. Schmidt, and D. Bonn, Europhys. Lett. **84**, 20006 (2008).
[42] J. R. Gomez-Solano, A. Petrosyan, S. Ciliberto, R. Chetrite, and K. Gawedski, Phys. Rev. Lett. **103**, 040601 (2009).
[43] J. Mehl, V. Blackly, U. Seifert, and C. Bechinger, Phys. Rev. E **82**, 032401 (2010).
[44] P. Martin, A. J. Hudspeth, and F. Jülicher, Proc. Natl. Acad. Sci. U. S. A. **98**, 14380 (2001).
[45] L. Dinis, P. Martin, J. Barral, J. Prost, and J.-F. Joanny, Phys. Rev. Lett. **109**, 160602 (2012).
[46] D. Mizuno, C. Tardin, C. F. Schmidt, and F. C. MacKintosh, Science **315**, 370 (2007).
[47] D. Mizuno, D. A. Head, F. C. MacKintosh, and C. F. Schmidt, Macromolecules **41**, 7194 (2008).
[48] M. Guo, A. J. Ehrlicher, M. H. Jensen, M. Renz, J. R. Moore, R. D. Goldman, J. Lippincott-Schwartz, F. C. MacKintosh, and D. A. Weitz, Cell **158**, 822 (2014).
[49] R. Zwanzig, J. Stat. Phys. **9**, 215 (1973).
[50] A. O. Caldeira and A. J. Leggett, Phys. Rev. Lett. **46**, 211 (1981).
[51] L. F. Cugliandolo and J. Kurchan, J. Phys. Soc. Jpn. **69**, 247 (2000).
[52] A. Crisanti, A. Puglisi, and D. Villamaina, Phys. Rev. E **85**, 061127 (2012).
[53] H. Risken, *The Fokker-Planck Equation* (Springer, Berlin, 1984).
[54] J. C. Cochran, Biophys. Rev. **7**, 269 (2015).
[55] T. Odijk, Macromolecules **16**, 1340 (1983).